Research Article

Journal of Environmental Nanotechnology

Nano-sulfonated Graphene Oxide: A Metal-free Catalyst for the Synthesis of Benzimidazoles and Antimicrobial Activities

V. Murali Krishna Madasu[1], M. Padma[1], Jyotsna Cherukuri[2], Kadali Yashoda[3], E. Vijaya[4], Ch. Praveen[5] and Manuri Brahmayya[2*]

[1]Department of Engineering Chemistry, Andhra University College of Engineering, Andhra University, Visakhapatnam, AP, India
[2]Department of Chemistry, VNR Vignana Jyothi Institute of Engineering and Technology, Hyderabad, TG, India
[3]Department of Chemistry, Vignan Institute of Information Technology (A), Duvvada, Visakhapatnam, AP, India
[4]Department of H and S, CMR Technical Campus, Hyderabad, TG, India
[5]Department of Chemistry, Pithapur Rajah's Government College(A), Kakinada, AP, India
Received: 03.11.2025 Accepted: 24.12.2025 Published: 30.03.2026
*brahma.orgchem@gmail.com

ABSTRACT

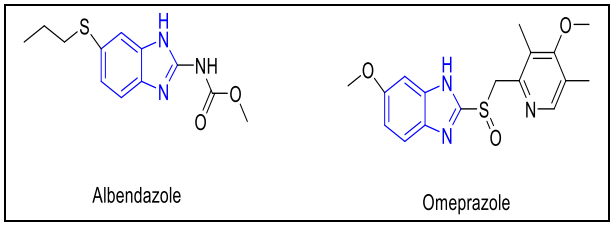
Nano sulfonated graphene oxide (SGO) was synthesized with slight modifications to previously reported methods. An efficient and ecofriendly protocol was developed for the synthesis of benzimidazole derivatives using *o*-phenylenediamine and D-glucose as substrates, employing a metal-free sulfonated graphene oxide carbocatalyst. A diverse range of benzimidazole derivatives was obtained in moderate to high yields (up to 94%) using a sustainable and readily available C1 source under sonication conditions. The reaction, carried out in ethanol with *tertiary*-butyl hydroperoxide, provides a general and novel approach for benzimidazole synthesis *via* a carbonylation pathway. The process is facilitated by a cost-effective and environmentally benign SGO nanocatalyst, enabling the formation of valuable products in excellent yields. The synthesized benzimidazole derivatives exhibited strong antibacterial activity, with inhibition rates of 99% to 100% against *Escherichia coli*, *Staphylococcus aureus*, *Pseudomonas aeruginosa*, and *Streptococcus pyogenes*.

Keywords: Sulfonated graphene oxide; *o*-phenylenediamines; D-glucose; Catalysis; Cyclization; Benzimidazoles.

1.INTRODUCTION

The one carbon chemistry (C1 source) has developed into an efficient method for the straightforward execution of single carbon homologation reactions in modern organic transformations. Some examples include CO (carbon monoxide) (Peng *et al.* 2019; Kang *et al.* 2018 and Ryu *et al.* 2015), carbon dioxide (CO_2) (Wang and Xi, 2019), paraformaldehyde (Natte *et al.* 2017), isocyanides (RNC) (Senadi *et al.* 2017), trialkyl amines (Xu *et al.* 2018), trialkyl orthoformate (Gaudino *et al.* 2017), formic acid (Wei *et al.* 2014), chlorodifluoromethane (Ma *et al.* 2019), and peroxides (Zhang *et al.* 2008). Similarly, solvents such as methanol (Liu *et al.* 2017), dimethylformamide (DMF) (Ding and Jiao, 2012), dimethyl sulfoxide (DMSO) (Huang *et al.* 2021), ethers (Mutra *et al.* 2018), and ethylene glycol (Kudale and Wang, 2020) utilized for the incorporation of CHO, CN, CH, CH_2, and CH_3 units are of paramount importance due to their cost-effectiveness, readily accessible feedstocks, and non-toxic nature. Although these methodologies are well established, many of them rely on transition metal catalysts, harsh reaction conditions, toxic reagents, and volatile organic solvents, which raise significant concerns regarding sustainability, cost, and environmental impact. In addition, the use of non-renewable C1 sources further limits their applicability in green chemistry frameworks.

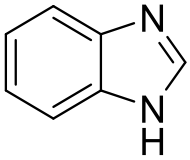
Benzimidazoles represent a significant class of N-heterocyclic compounds exhibiting diverse biological properties (Refat *et al.* 2021; Francesconi *et al.* 2020; Barker *et al.* 1960; Desai *et al.* 2012 and Rajora and Srivastava, 2009)). Notably, the medicinal attributes of benzimidazole derivatives have garnered considerable attention in the medical field due to their antimicrobial, antihistaminic, proton pump inhibitory, anti-inflammatory, and antihypertensive effects (Desai *et al.* 2014). Furthermore, benzimidazoles address mitochondrial dysfunction for Alzheimer's disease and possess psychoactive, anticoagulant, and analgesic properties, proving to be valuable agents in the management of diabetes mellitus (Marinescu *et al.* 2021; Bansal and Silakari, 2012).



The organic moiety was found in some of the clinical drugs such as Albendazole is an anthelmintic drug and Omeprazole is an Anti-ulcer drug.

There are numerous synthetic methodologies reported for the preparation of benzimidazole scaffolds (Alminderej and Lotfi, 2021; Mahesh *et al.* 2016; Hati *et al.* 2016; Baars *et al.* 2014 and Lin *et al.* 2014). Among these, the reaction of *o*-phenylenediamine derivatives with different one-carbon sources such as aldehydes (Li *et al.* 2019) (shown in Scheme.1a), carboxylic acids (Dudd *et al.* 2003), N, N-Dimethylformamide (Kattimani *et al.* 2015), β-di ketones (Mayo *et al.* 2014), ortho esters (Bastug *et al.* 2012), alkyl amines, benzyl amines (Nguyen *et al.* 2013; Nguyen *et al.* 2012) (Scheme. 1b,1c), alcohols (Krishna *et al.* 2025; Sun *et al.* 2015) (Scheme. 1d,1e), and carbon dioxide (Zhang *et al.* 2016; Hao *et al.* 2014) (Scheme. 1f,1g), Benzimidazolones (Kovvuri *et al.* 2016; Yu *et al.* 2013; Brahmayya *et al* 2017 and Chen *et al.* 2008) (Scheme. 1h,1i) have emerged as a particularly significant approach under a variety of reaction conditions. Despite their synthetic utility, several of these protocols suffer from notable drawbacks, including the use of cost expensive, toxic metal catalysts, strong inorganic bases, non-renewable C1 source, and VOCs as solvents, thereby limiting their sustainability and practical applicability.

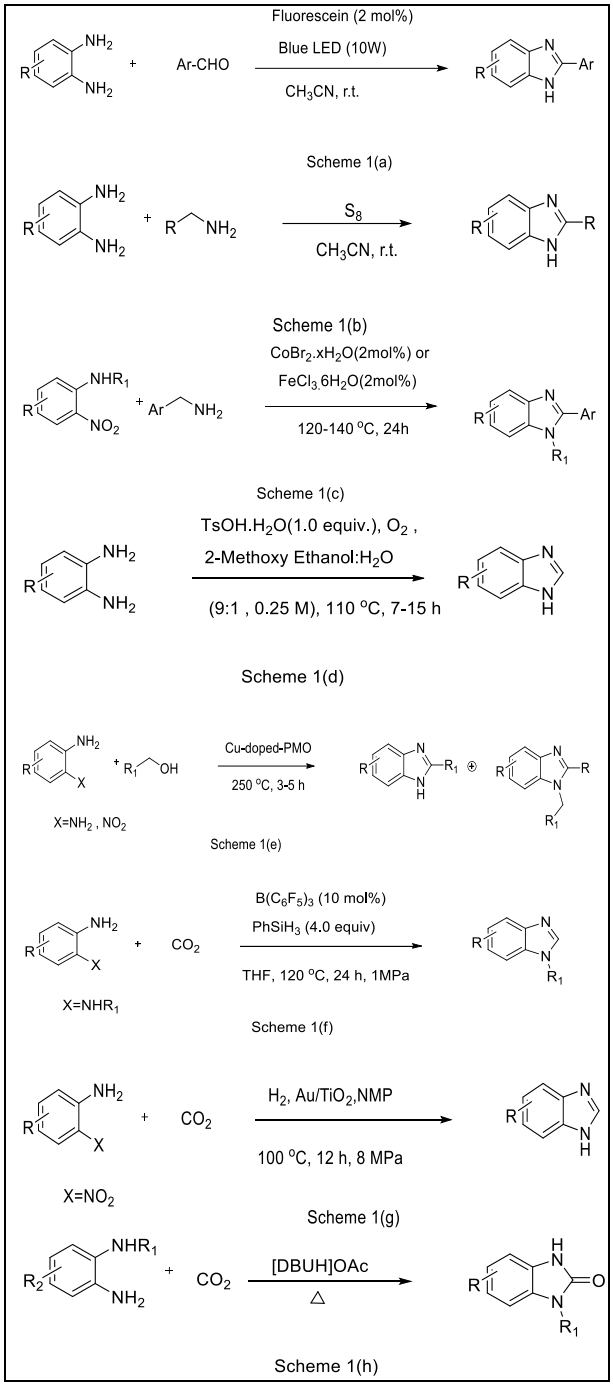
Recent advances in catalysis have emphasized the importance of metal-free and carbon-based nanocatalysts as sustainable alternatives to traditional metal systems. Among these, sulfonated graphene oxide (SGO) has emerged as a promising heterogeneous catalyst due to its high surface area, strong Brønsted acidity (Sulfonated groups), excellent dispersibility in aqueous media, and recyclability. Despite these advantages, the application of SGO in the synthesis of benzimidazoles remains relatively underexplored, particularly in the context of biomass-derived substrates and green reaction media.

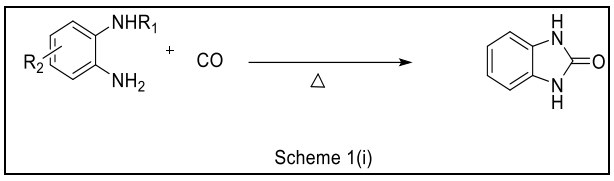


Benzimidazole

From the past few decades, glucose has been identified as one of the highly abundant and versatile six-carbon biomass derived feedstocks, owing to its ready availability, low cost, and strategic importance as a renewable one of the starting material for the preparation of diverse chemical entities (Li *et al.* 2020). Growing societal and regulatory emphasis on environmentally benign and economically sustainable chemical processes has prompted the exploration of C5/C6 sugars as key substances for the construction of biologically active heterocyclic small molecules. In this context, we report a previously unrecognized strategy for the *in situ* development of a methine (–CH–) unit from D-glucose with mild, metal-free ambient reaction conditions in aqueous media (Li and Chen, 2006). The synthetic possibility of this method is validated through the formation of C–N bond during the oxidative cyclization of *o*-phenylenediamine, enabling efficient access to benzimidazole frameworks (Scheme 2).

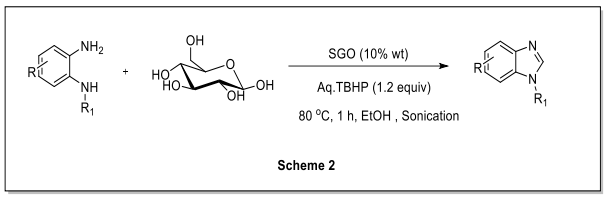
1.1 Past Work





Scheme 1(i)

1.2 Present Work



Scheme 2

2. EXPERIMENTAL PROCEDURE

2.1 Materials and Methods

The required raw chemicals, reagents, and solvents were supplied by commercial vendors and used exactly as given in the subsequent reactions without further purification. (Commercial providers provided the chemicals, reagents, and solvents needed for the procedure, which were then utilized in the subsequent processes without further purification.) All reactions were conducted in presence of inert N_2 atmosphere using oven-dried glassware. Using an Agilent LC-MSD mass spectrometer in conjunction with an Agilent 1200 Series Binary LC system, LC-MS analyses were acquired. Using a 400 MHz spectrometer (Gemini Varian), the ^{13}C and ^{1}H NMR spectral data were recorded. The Proton NMR and ^{13}C NMR spectra were acquired at an absolute temperature of 298 K. Chemical shift (δ values) readings are recorded using tetra methyl silane (TMS) or residual solvent as an internal standard solvent.

DMSO-d6 or $CDCl_3$ were employed as analytical solvents. A 400–500 mesh silica gel has been used in the column chromatography. By using X-ray diffraction (XRD) technique, the d-spacing of the catalyst was measured. The morphology images of the catalyst were captured by scanning electron microscopy and high-resolution transmission electron microscopy (HR TEM), Japan.

2.2 General Synthetic Procedure for SGO

SGO was synthesized accordingly the previous report (Brahmayya *et al.* 2018) with minor modifications. Graphene oxide (40 mg) was first mixed in 40 mL of deionized water in a round-bottom flask and stirred well at room temperature. The suspension was subsequently ultrasonicated at 40 kHz to achieve a homogenous dispersion. Then (repeated the word many times), a 0.2 g of sodium borohydride was added to the graphene oxide dispersion under alkaline conditions (pH = 10–11). The reaction mixture was heated to 80 °C, and the resulting partly reduced graphene oxide (rGO) was subsequently separated *via* centrifugation.

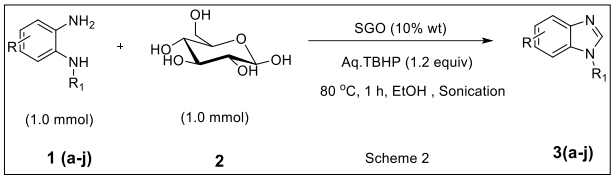
The obtained rGO was redispersed in 40 mL of distilled water and subsequently sonicated for 15–20 minutes in an ultrasonic bath, after which it was stored under refrigerated conditions. A diazonium salt was synthesized by reacting 40 mg of sulfanilic acid with 1.0 mL of 1 N HCl and 5.5 mL of water at 0 °C. The solution was further treated with potassium nitrite (14.5 mg) to finalize the diazotization process. The freshly made diazonium solution was added dropwise to the rGO dispersion at 0 °C, and the resultant mixture was stirred gently at room temperature for 10 hours to promote sulfonation.

The resultant black precipitate was isolated by centrifugation for 15 minutes and subsequently washed five times with distilled water to eliminate unreacted substances. The product was ultimately obtained using vacuum filtration and subsequently dried at 60 °C for 2–3 hours, yielding SGO.

2.3 General Experimental Procedure for the Cyclization of *o*-phenylenediamines with D-glucose to Benzimidazoles

A sustainable and environmentally benign single step procedure was developed for the preparation of benzimidazole derivatives (3a–3j). In a sealed 15 mL reaction tube, substrates (1a–1j) (1.0 mmol) were mixed with ethanol as the reaction medium (0.2 M), D-glucose (1.0 equivalent) as a renewable and non-toxic additive, *tertiary*-butyl hydroperoxide (TBHP) (70% aqueous solution, 1.0 mmol) as a green oxidant, and a catalyst amount of SGO (0.2 mg). This reaction mixture was placed at 80°C under solvent-safe sonication conditions and monitored by thin-layer chromatography. The reaction completed in approximately 1 hour. Once the reaction completed, it was allowed to cool to room temperature and dissolved in DI water. The quenching was achieved using sodium bicarbonate, avoiding harsh acidic or basic work-up conditions. The anticipated product was isolated and accomplished through ethyl acetate extraction.

Desired compounds were purified by column chromatography with a 1:1 mobile phase mixture of ethyl acetate and *n*-hexane. This protocol emphasizes metal-free catalysis, aqueous reaction media, renewable additives, and minimal waste generation, demonstrating its alignment with green chemistry principles and suitability for sustainable heterocyclic synthesis. The compounds were characterised by the ^{1}HNMR and ^{13}CNMR, FTIR, High Resolution Mass spectroscopic techniques (HRMS).



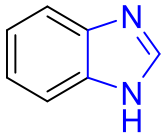
2.3.1 Compound (3a): 1H-benzo[*d*]imidazole

The characterization data obtained for 1*H*-benzo[*d*]imidazole were identical to those reported previously (Kovvuri *et al.* 2016; Yu *et al.* 2013; Brahmayya *et al* 2017).

Yield 91%; white solid; m.p 166–168 0C;

HRMS (ES +) calcd. for $C_7H_6N_2$ $[M + H]^+$: 119.05; found: 119.02 FTIR ν_{max}/cm^{-1}: 3145, 1640, 1585, 1302, 1232, 730. ^{1}HNMR (300 MHz, DMSO-d6): δ 6.82 (s, H), 6.43 (s, 2H), 6.03 (m, 2H), 5.38 (s, 1H). ^{13}CNMR (100 MHz, DMSO-d6): δ 141.1, 137.18, 122.6, 115.15.

MS (EI, 70 eV): m/z (%):118.02 (M^+,100), 91.06 (26), 79 (42), 63 (62).



Compound (3a):1H-benzo[d]imidazole

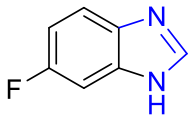
2.3.2 Compound 3(b): 6-fluoro-1*H*-benzo[*d*]imidazole

The characterization data obtained for 6-fluoro-1H-benzo[*d*]imidazole were identical to those previously reported (Kovvuri *et al.* 2016; Yu *et al.* 2013; Brahmayya *et al* 2017).

Yield 93%; white crystalline solid; mp 91–94 ^{0}C; HRMS (ES +) calcd. for $C_7H_5FN_2$ $[M + H]^+$: 137.04; found: 137.06

FTIR ν_{max}/cm^{-1}: 3100–2495, 1662, 1580, 1310, 1201, 750. ^{1}HNMR (300 MHz, DMSO-d_6): δ 8.16 (s, 1H), 7.46 (dd, J =8.5, 4.4 Hz, 1xH), 7.27 (d,J =3.2 Hz, 1H), 6.95 (dt, J = 8.9 Hz, 2.0 Hz, 1H), 5.32 (s, 1xH). ^{13}C NMR (100MHz, DMSO-d_6): δ 160.01(d, J_{C-F} = 234.5 Hz), 157.03(s), 143.1(s), 115.10(d, J_{C-F} = 9.7 Hz), 112.30 (d, J_{C-F} = 24.5 Hz), 102.15 (d, J_{C-F} = 25.3 Hz).

MS (EI, 70 eV): m/z (%):136.04 (M^+, 100), 124.5 (45), 124 (18), 95 (42), 75 (17), 68 (14).



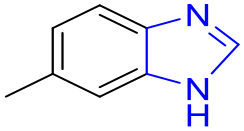
compound 3(b): 6-fluoro-1*H*-benzo[*d*]imidazole

2.3.3 Compound (3c): 6-methyl-1H-benzo[*d*]imidazole

The characterization data obtained for 6-methyl-1*H*-benzo[*d*]imidazole were identical to those previously reported (Kovvuri *et al.* 2016; Yu *et al.* 2013; Brahmayya *et al* 2017).

Yield 87%; whitish brown solid; m. p 124–126 ^{0}C; HRMS (ES +) calcd. for $C_8H_8N_2$ $[M + H]^+$: 133.07; found: 133.05

FTIR ν_{max}/cm^{-1}: 2982, 1684, 1486, 1332, 1076, 1019, 883, 741, 663. ^{1}HNMR (300 MHz, DMSO-d_6): δ 9.59 (s,1H), 7.96 (d, J = 8.5 Hz, 1H), 7.34 (s, 1H), 7.54 (d, J = 8.6 Hz, 1H), 3.12 (s, 3H). ^{13}CNMR (100 MHz, DMSO-d_6): δ 144.01, 138.08, 136.50, 133.02, 122.10, 116.80, 115.60, 21.30. MS (EI, 70 eV): m/z (%); 132.07 (M^+, 100), 131 (84), 102 (20), 76 (29), 65 (13), 94 (16).



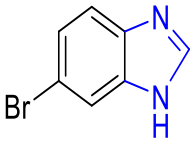
compound (3c) 6-methyl-1*H*-benzo[*d*]imidazole

2.3.4 Compound (3d): 6-bromo-1*H*-benzo[*d*]imidazole

The characterization data obtained for 6-bromo-1*H*-benzo[*d*]imidazole were identical to those previously reported (Kovvuri *et al.* 2016; Yu *et al.* 2013; Brahmayya *et al* 2017).

Yield 88%; white crystalline solid; mp 141–143 ^{0}C; HRMS (ES +) calcd. for $C_7H_5BrN_2$ $[M + H]^+$: 196.96; found: 197.06

FTIR ν_{max}/cm^{-1}: 3509, 3149, 3185, 1621, 1439, 740. ^{1}H NMR (300 MHz, DMSO-d_6): δ 8.53 (s, 1H), 7.23 (s, 1H), 7.55 (d, J = 8.5 Hz, 1H), 7.33(d, J = 8.6 Hz, 1H). ^{13}C NMR (100MHz, DMSO-d_6): δ 143.10, 135.00, 136.60, 125.71, 119.10, 118.20, 117.89. MS (EI, 70 eV): m/z (%): 195.96 (M^+, 100), 120.5 (46), 118 (17), 94 (42), 80 (18), 70 (15).



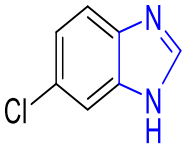
Compound (3d): 6-bromo-1*H*-benzo[*d*]imidazole

2.3.5 Compound (3e): 6-chloro-1*H*-benzo[*d*]imidazole

The characterization data obtained for 6-chloro-*1H-benzo [d]*imidazole were identical to those previously reported (Kovvuri *et al.* 2016; Yu *et al.* 2013; Brahmayya *et al.* 2017).

Yield 90%; whitish solid; m. p 118–120 ^{0}C; HRMS (ES +) calcd. for $C_7H_5ClN_2$ [M + H]$^+$: 153.01; found: 153.02

FTIR ν_{max}/cm^{-1}: 2999, 1670, 1480, 1323, 1076, 1021, 883, 740, 660. ^{1}H NMR (300 MHz, DMSO-d_6): δ 8.74 (s, 1H), 7.55 (s, 1H), 7.23 (d, J = 8.5 Hz, 1H), 7.49 (d, J = 8.4 Hz, 1H). ^{13}C NMR (101 MHz, DMSO-d_6): δ 145.11, 140.45, 137.00, 126.88, 122.00, 115.23, 114.8. MS (EI, 70 eV): m/z (%):152.01 (M$^+$, 100), 124 (47), 123 (20), 94 (41), 78 (19), 70 (18).



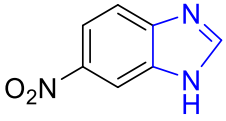
Compound (3e): 6-chloro-1*H*-benzo[*d*]imidazole

2.3.6 Compound (3f); 6-nitro-1*H*-benzo[*d*]imidazole

The characterization data obtained for 6-nitro-1*H*-benzo[*d*]imidazole were identical to those previously reported (Kovvuri *et al.* 2016; Yu *et al.* 2013; Brahmayya *et al* 2017).

Yield 88%; whitish solid; m. p 195–196 ^{0}C; HRMS (ES +) calcd. for $C_7H_5N_3O_2$ [M + H]$^+$: 164.04; found: 164.02

FTIR ν_{max}/cm^{-1}: 2984, 1678, 1486, 1333, 1067, 1039, 883, 741, 663. ^{1}HNMR (300 MHz, DMSO-d_6): δ 12.64 (s, 1H), 8.76 (s, 1H), 8.64 (s, 1H), 8.24 (d, J = 8.5 Hz, 1H), 7.21 (d, J = 8.6 Hz, 1H). ^{13}C NMR (101 MHz, DMSO-d_6): δ 148.03, 144.50, 119.60. MS (EI, 70 eV): m/z (%):163.04 (M$^+$, 100), 148 (50), 137(48), 122 (18), 105 (82), 79 (39), 78 (20), 78 (16), 67 (17), 56 (17), 53 (27), 51 (15).



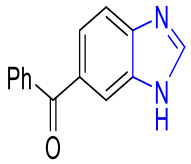
Compound (3f); 6-nitro-1*H*-benzo[*d*]imidazole

2.3.7 Compound (3g): (1*H*-benzo[*d*]imidazol-6-yl)(phenyl) methanone

The characterization data obtained for (1*H*-benzo[*d*]imidazol-6-yl) (phenyl) methanone were identical to those previously reported (Kovvuri *et al.* 2016; Yu *et al.* 2013; Brahmayya *et al.* 2017).

Yield 91%; yellow crystalline solid; m.p 144–146 ^{0}C; HRMS (ES +) calcd. for $C_{14}H_{10}N_2O$ [M + H]$^+$: 224.08; found: 224.05

FTIR ν_{max}/cm^{-1}: 2989, 2854, 1687, 1476, 1342, 1041, 1029, 870, 746, 651. ^{1}H NMR (300 MHz, DMSO-d6): δ 8.29 (s, 1H), 7.88 (s, 1H), 7.76 (m, 5H), 7.61(t, J =7.5, 1.1 Hz, 2H). ^{13}C NMR (100 MHz, DMSO d_6): δ 198.00, 146.01, 148.50, 137.10, 132.11, 130.80, 129.11, 126.13, 125.37, 117.12, 114.81. MS (EI, 70 eV): m/z (%): 190.07 (M$^+$, 100), 138 (49), 120 (20), 107 (84), 80 (40), 79 (18), 77 (17), 69 (16), 58 (19), 55 (30), 52 (16).



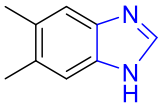
Compound (3g): (1*H*-benzo[*d*]imidazol-6-yl)(phenyl)methanone

2.3.8 Compound (3h): 5,6-dimethyl-1*H*-benzo[*d*]imidazole

The characterization data obtained for 5 Compound (3h) 5,6-dimethyl-1*H*-benzo[*d*]imidazole were identical to those previously reported (Kovvuri *et al.* 2016; Yu *et al.* 2013; Brahmayya *et al* 2017).

Yield 87%; whitish solid; m. p 190–192 ^{0}C; HRMS (ES +) calcd. for $C_9H_{10}N_2$ [M + H]$^+$: 147.08; found: 147.09

FTIR ν_{max}/ cm^{-1}: 3000, 2950, 1676, 1489, 1341, 1045, 1026, 870, 742, 673. ^{1}HNMR (300 MHz, DMSO-d6): δ 7.76 (s, 1H), 7.68 (s, 2H), 4.29 (s, 1H), 2.41 (s, 6H). ^{13}C NMR (100 MHz, DMSO-d_6): δ 141.68, 137.84, 132.44, 114.98, 21.89. MS (EI, 70 eV): m/z(%); 146.08 (M$^+$, 100), 118 (20), 100 (32), 105 (13), 94 (16), 93 (8), 66 (13).



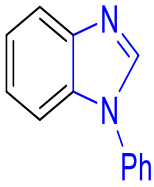
Compound (3h): 5,6-dimethyl-1*H*-benzo[*d*]imidazole

2.3.9 Compound (3i): 1-phenyl-1*H*-benzo[*d*]imidazole

The characterization data obtained for Compound (3i): 1-phenyl-1*H*-benzo[*d*]imidazole were identical to those previously reported (Kovvuri *et al.* 2016; Yu *et al.* 2013; Brahmayya *et al* 2017).

Yield is 92%; white solid; m.p 196–199 ^{0}C; HRMS (ES+) calcd. for $C_{13}H_{10}N_2$ [M + H]$^+$: 195.08; found: 196.01

FTIR ν_{max}/cm^{-1}: 3150-2500, 1658, 1576, 1311, 1235, 748. ^{1}HNMR (300 MHz, DMSO-d_6): δ 8.14 (s, 1H), 7.49–7.80 (m, 1H), 7.58 (m, 5H), 7.45 (dd, J = 10.5, 4.3 Hz, 1H). ^{13}C NMR (100 MHz, DMSO-d_6): δ 155.71(CO), 133.90, 132.50, 130.00, 128.00, 126.00, 126.00, 124.00, 143.10, 142.00, 135.66, 132.90, 129.77, 128.6, 123.23, 122.10, 121.40, 111.4. MS (EI, 70 eV): m/z (%): 194.08 (M+, 100), 120 (20), 118 (17), 105 (12), 92 (13), 91 (9), 65 (11).



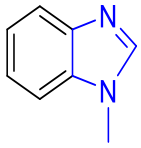
Compound (3i): 1-phenyl-1*H*-benzo[*d*]imidazole

2.3.10 Compound (3j): 1-methyl-1*H*-benzo[*d*]imidazole

The characterization data obtained for 1-methyl-1*H*-benzo[*d*]imidazole were identical to those previously reported (Kovvuri *et al.* 2016; Yu *et al.* 2013; Brahmayya *et al* 2017).

Yield 88%; whitish solid; m.p 193–195 ^{0}C; HRMS (ES +) calcd. for $C_8H_8N_2$ [M + H]$^+$: 133.07; found: 133.05

FTIR ν_{max}/cm^{-1}: 3150–2480, 2859, 1650, 1599, 1310, 1234, 745. ^{1}H NMR (300 MHz, $CDCl_3$): δ 8.52 (s, 1H), 7.79 (s, 1H), 7.44 (d, J = 7.3 Hz, 1H), 7.30 (m, 2H), 3.90 (s, 3H). ^{13}CNMR (100 MHz, $CDCl_3$): δ 145.30, 135.00, 123.00, 122.50, 118.68, 109.88, 32.10. MS (EI, 70 eV): m/z (%): 132.07 (M$^+$, 100), 131 (37), 120 (17), 118 (13), 105 (12), 93 (17), 92 (10), 65 (19).



Compound (3j): 1-methyl-1*H*-benzo[*d*]imidazole

2.4 Antimicrobial Activities

Cultures of *P. aeruginosa*, *E. coli*, *S. aureus*, *S. pyogenes* and *Luria bertani* broth were diluted to OD600 of 0.1 to 100 µL at 37 ºC. It was anticipated that organic samples at a certain concentration will self-regulate after the cell suspension was added to 100 µL of medium overnight (Hao *et al.* 2014). The solutions were subjected to 365 nm radiation for 15 minutes before the cell suspension was added in order to control the antibacterial activity. The cells were subsequently incubated at 37 °C on a microtiter plate. Over a 12-hour period, optical density at 600 nm (OD_{600}) was measured every 10-15 minutes to track cell growth. A 30-second shaking interval was conducted before to each measurement. The initial OD_{600} number at time zero was deducted to normalize the data.

3. RESULTS AND DISCUSSION

3.1. Catalyst Optimization

The experiment started with *o*-phenylenediamine (1a) (1.0 mmol) and D-glucose (3.0 equivalents), with TBHP (70% in EtOH) (2.0 equivalents) in ethanol at 80 °C for 1 hour. The target 3a was formed with a yield of < 1% (Table 1, item 1). The procedure was carried out with different Brønsted acids, like $BF_3{\cdot}Et_2O$, graphite, and graphene as additives to enhance the nature of ring opening in glucose at different temperatures (Table 1, item 2-14). Sulfonated graphene oxide had an exceptional yield of 94% (Table 1, item 17). The use of different oxidants, including H_2O_2, CH_3CN, and toluene, did not increase the yield (Table 1, item 13, 14, 21, 23-25). Increasing the amount of SGO from 5.0 mg to 10.0 mg, improves product yields from 57% to 94% (Table 1, item 15, 16, 17). Modifying the reaction time and temperature decreased the product yields (Table 1, items 18−25).

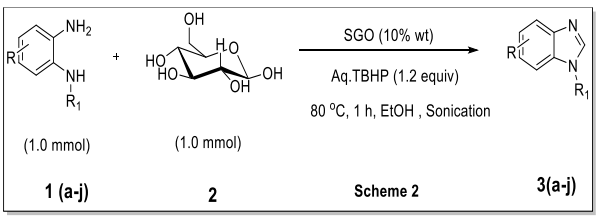


Table 1. Optimization of the catalyst SGO

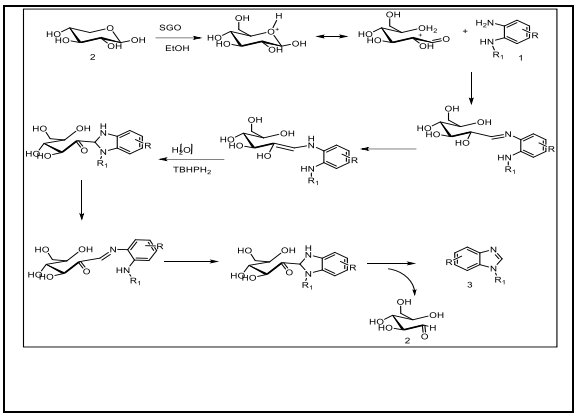
Entry	[a]Catalyst/ acid	Oxidant	T (ºC)	[b]Yield (%)
1	–	TBHP	RT	<1
2	Hydrochloric acid	TBHP	RT	1–3
3	Hydrochloric acid	TBHP	30	6
4	Hydrochloric acid	TBHP	50	> 6
5	*p*-Toluene sulfonic	TBHP	30	>7
6	$BF_3 \cdot Et_2O$	TBHP	30	>1–3
7	Graphite	TBHP	30	> 8
8	Graphene	TBHP	30	> 10
9	Graphite	TBHP	45	>10
10	Graphene	TBHP	45	>10
11	Grapheneoxide	TBHP	30	>11
12	Grapheneoxide	TBHP	45	>11
13	Grapheneoxide	H_2O_2	30	> 7
14	Grapheneoxide	Toluene	45	> 7
15	SGO (5 mg)	TBHP	30	57
16	SGO (7.5mg)	TBHP	45	79
17	SGO (10mg)	TBHP	80	94
18	0	TBHP	80	0
19	SGO (7.5mg)	TBHP	60	75
20	SGO (5 mg)	TBHP	80	50
21	SGO (7.5mg)	Toluene	80	87
22	SGO (10mg)	TBHP	80	90
23	SGO (5 mg)	Acetonitril	30	69
24	SGO (7.5mg)	Acetonitril	45	78
25	SGO (10mg)	Acetonitri	80	80

[a]A mixture of 1a (1.00 mmol), and SGO (10 Wt %) in the solvent (5–10 ml) was stirred at the mentioned temperature

[b]Isolated product yield

3.2 Viable Pathway

The SGO-catalyzed oxidative cyclization of *o*-phenylenediamines with glucose proceeds *via* a surface-assisted, metal-free mechanism, where glucose acts as a renewable C1 source. Initially, glucose interacts with the –sulfonated funtions of SGO, undergoing activation and transformation into an *in situ* electrophilic methine equivalent. One amino group of *o*-phenylenediamine attacks this species to form an intermediate, which upon dehydration generates an imine. Subsequent intramolecular cyclization yields a dihydrobenzimidazole intermediate. Finally, oxidative aromatization using TBHP in ethanol produces the benzimidazole derivative, with SGO facilitating peroxide activation and stabilizing intermediates. Ultrasonic irradiation enhances mass transfer and accelerates the reaction. Overall, this strategy enables efficient dual C–N bond formation under green and metal-free conditions.



Scheme. 3 Plausible mechanisms of cyclization of o-phenylenediamines with glucose

3.3 Acidic Characteristics of SGO

About 50 mg of SGO and 50 mL of the inorganic base solvent (0.01 mol/L NaOH, 0.01 mol / L Na_2CO_3) were taken in a 250 mL volumetric flask, then the mixture was stirred for at least 2 hours (Krishna *et al.* 2025). Methyl red was utilized as the indicator, and 10 mL aliquots were employed to titrate each reaction base. For the titration, 0.010 mol/L HCl was used (Brahmayya *et al.* 2017). The number of acidic functional groups in mmol per gram of SGO was calculated using the following equation.

$$NSF = CHI\ (V_{HCL}{-}B,\ Pre{-}V_{HCL}{-}B,\ Post)$$

$$M_{SGO}$$

N_{SF} = Quantity of surface functionality.

C_{HCl} = Concentration of the HCl titrant.

$V_{HCl\ B,\ Before}$= Volume of the HCl for the pre-reaction base.

$V_{HCl\ B,\ After}$ = Volume of the HCl for the post-reaction base.

M_{SGO}=Effective mass of the SGO.

The concentration of carboxyl groups, expressed in terms of mmol/g rather than as an exact count per sheet due to the non-stoichiometric and variable nature of the material, was determined to be 3.11 mmol/g.

On the other hand, the concentration of the sulfonyl groups were found that 7.89 mmol/g and phenolic groups concentration was determined as 2.33 mmol/g. Through EDX analysis of the S content, the number of sulfonic functions was ascertained (Refat *et al.*

2021). The concentration of carboxyl groups were calculated by subtracting the concentration of sulfonic groups from the results of the $NaHCO_3$ titration. The concentration of phenolic groups were measured by subtracting the concentrations of carboxyl and sulfonic groups from the results of the Na_2CO_3 titration.

Thus the prepared SGO was also well characterized by various analytical techniques like XRD, SEM, EDX (Section.3.4) for its newly introduced SGO functions. It is noticed that SGO's sulphur atomic percentage was observed 8.27% Fig.4(b). Coincidentally, this is almost equal to the concentration of the sulfonyl group concentrations 7.89 mmol/g. Thus, the 2D structure of SGO and its high acidic sites contributing to superior catalytic performance at different optimized reaction conditions (Catalyst Optimization Table 1) for the selected organic substrates to convert to heterocyclic molecules and thus efficiently acted as metal free nano carbon catalyst in the preparation of the benzimidazoles heterocyclic compounds under the moderate reaction conditions (Yu *et al.* 2008; Cao *et al.* 2018 and Mohammadi *et al.* 2017).

3.4 Morphological Analysis of SGO

The SEM and TEM techniques were used to analyze the morphological characteristics of GO and SGO, as shown in Figures 1(a,b) and 2(a,b). The SEM micrographs exhibit a distinctive wrinkled, sheet-like appearance, validating that the layered morphology of GO nanosheets was preserved post-sulfonation (Daripa *et al.* 2020). The lateral dimensions of the SGO sheets were determined to be around 2.5–5 µm in width and 6–8 µm in length. The mean thickness of the SGO nanosheets was determined to be approximately 1.7 nm, attributable to the partial restacking of graphene oxide layers induced by π–π interactions during the sulfonation functionalization process.

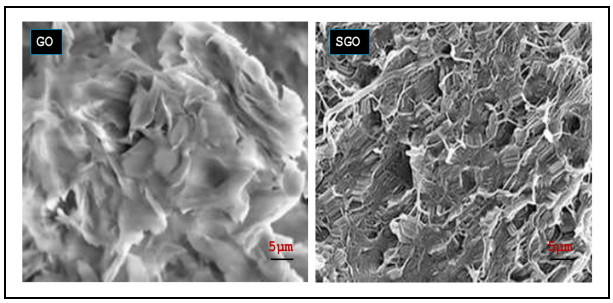


Fig. 1: SEM photographs of (a) GO and (b) SGO

The maintenance of this two-dimensional configuration is beneficial for acid-catalyzed reactions, since reactant molecules can easily reach and engage with the acidic functional groups exposed on both surfaces of the SGO nanosheets. Furthermore, EDS analysis of GO (Figure 3a) and SGO (Figure 3b) verified the presence of C, O, and S elements. Elemental mapping was utilized to evaluate the spatial distribution of carbon in GO (Figure 4a) and sulfur in SGO (Figure 4b), demonstrating a homogeneous distribution of aryl-sulfonyl groups throughout the SGO surface (Farid *et al.* 2025; Farid *et al.* 2020; Zahid *et al.* 2021; Tchekep *et al.* 2024 and Azmiyawati *et al.* 2025).

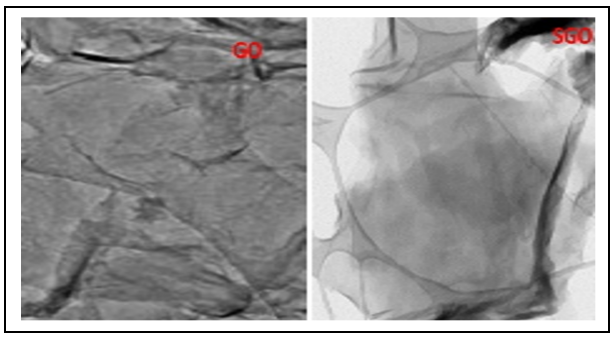


Fig. 2: TEM photographs of (a) GO and (b) SGO

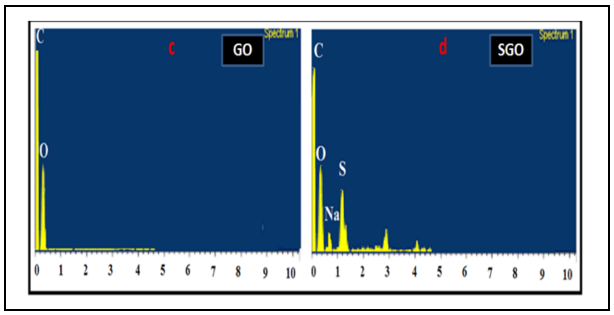
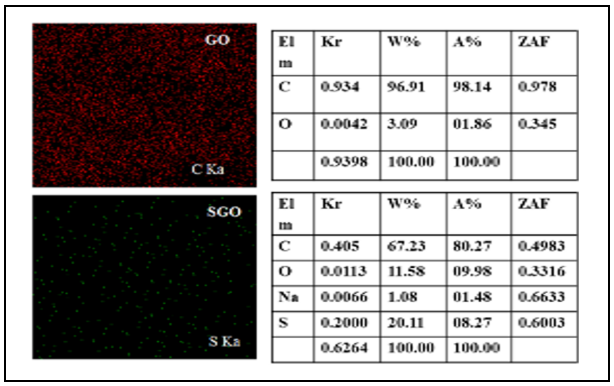


Fig. 3: EDS spectrum of (a) GO and (b) SGO



Elm	Kr	W%	A%	ZAF
C	0.934	96.91	98.14	0.978
O	0.0042	3.09	01.86	0.345
	0.9398	100.00	100.00	

Elm	Kr	W%	A%	ZAF
C	0.405	67.23	80.27	0.4983
O	0.0113	11.58	09.98	0.3316
Na	0.0066	1.08	01.48	0.6633
S	0.2000	20.11	08.27	0.6003
	0.6264	100.00	100.00	

Fig. 4: Elemental mapping of (a) GO and (b) SGO

The EDS elemental analysis revealed that the sulfur content in the synthesized SGO was 8.27 at.% (20.11 wt.%), exceeding the previously reported values (Azmiyawati *et al.* 2025). The atomic sulfur-to-carbon (S/C) ratio was found to be 0.103, supporting the successful integration of sulfonic acid functions onto the graphene oxide surface (Cao *et al.* 2018; Daripa *et al.* 2020; Basak *et al.* 2020 and Azmiyawati *et al.* 2025) Raman spectroscopic study (Figure 5) confirmed an increase in the ID/IG ratio from 1.41 for GO to 2.09 for SGO, signifying an increase in structural disorder. This

modification indicates the partial elimination of oxygen-containing functional groups from the GO surface during $NaBH_4$ treatment, resulting in the synthesis of sulfonated graphene-based nanomaterials (Cao *et al.* 2018; Mohammadi *et al.* 2017).

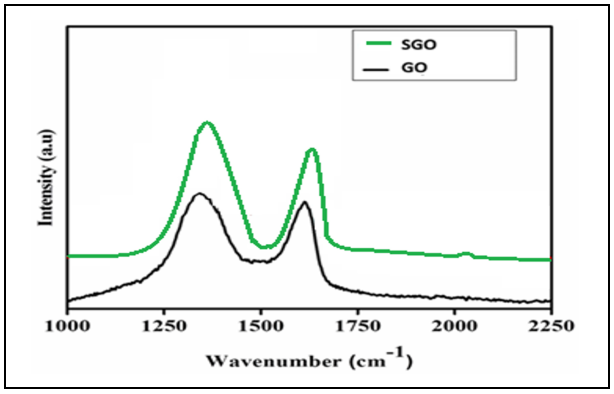


Fig. 5: Raman spectra for GO and SGO

X-ray diffraction (XRD) patterns confirmed the structural alteration. The characteristic GO diffraction peak at 2θ = 12.5° (interlayer spacing = 6.89 Å), shown in Figure 6(a), shifted to 2θ = 26.2° (interlayer spacing = 3.29 Å), as shown in Figure 6(b), following sulfonation (SGO). This change indicates the restacking and restructuring of graphene oxide layers due to strengthened π–π interactions induced by the sulfonation process (Daripa *et al.* 2020).

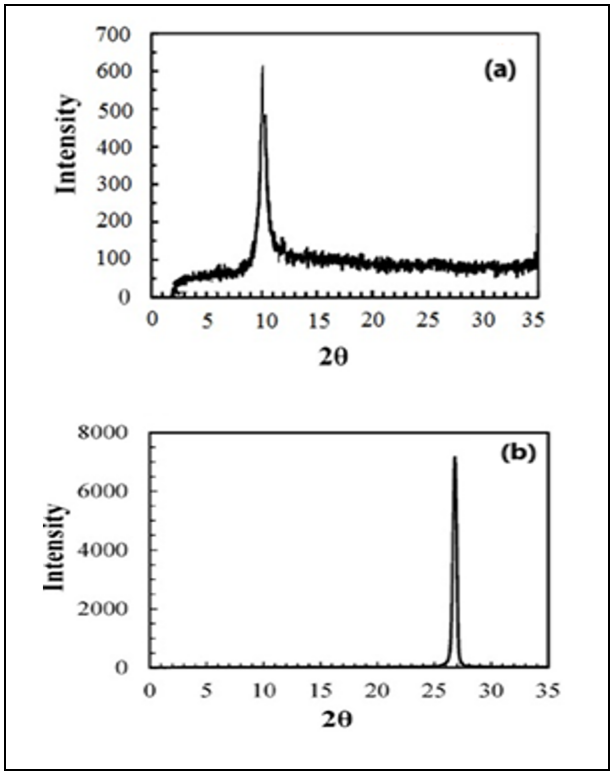


Fig. 6: XRD patterns for the (a)GO and (b)SGO

The thermal stability of SGO was investigated using thermogravimetric analysis (TGA) (Figure 7). The TGA profile confirmed an initial mass loss of almost 10% between 160–180 °C, attributable to the elimination of physically adsorbed and intercalated water molecules (Azmiyawati *et al.* 2025) A considerable weight reduction of around 30% seen between 180 and 220 °C correlates with the disintegration of oxygenated functional groups, including carbonyl and carboxyl species. The ensuing progressive mass loss beyond 220 °C is attributed to the thermal breakdown and liberation of sulfonic acid groups from the SGO surface (Garfunkle *et al.* 2008). After comprehensive structural and thermal characterization of GO and SGO, the catalytic efficacy of the synthesized SGO was determined for the cyclization of diacylhydrazines.

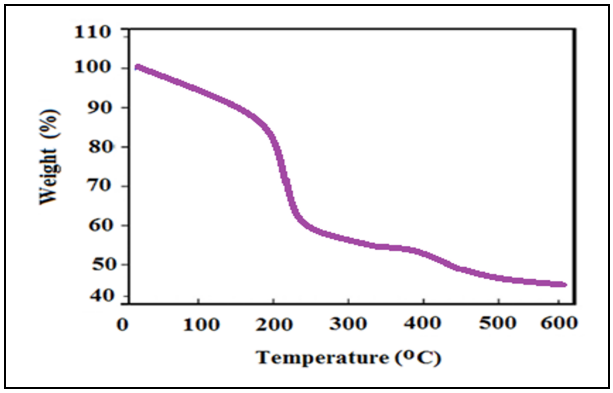


Fig. 7: Thermogravimetric analysis of the SGO

3.5 UV- visible Analysis of SGO

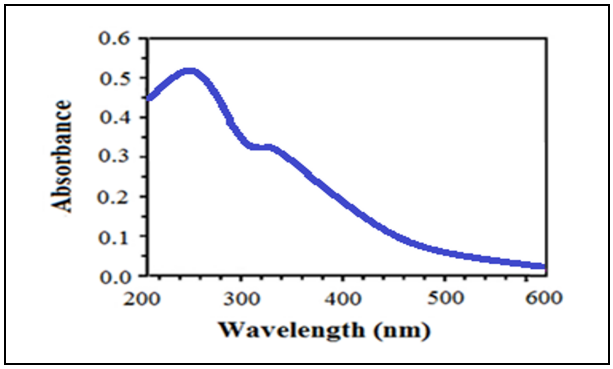


Fig. 8: UV -visible analysis of SGO

Figure 8 shows the UV–visible absorption spectrum of sulfonated graphene oxide dispersed in water at a concentration of 0.20 g L^{-1}. The SGO nanocatalyst exhibits a significant absorption band at 229 nm, ascribed to π→π* electronic transitions linked to the conjugated aromatic C=C structure. A reduced absorption characteristic at about 296 nm is attributed to n→π* transitions of nonbonding electrons in oxygen-containing groups, including carboxylic carbonyl (O=C-) and

hydroxyl (–OH) functionalities (Brahmayya *et al.* 2015; Khan *et al.* 2005).

4.1 Reaction Scope and Discussion

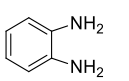
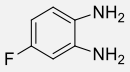
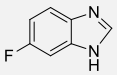
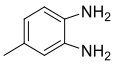
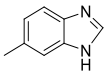
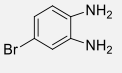
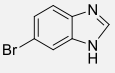
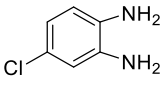
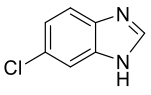
The generality and robustness of the present SGO catalyzed oxidative cyclization protocol were evaluated using a broad range of *o*-phenylenediamine derivatives (1a–j, Table-2) bearing diverse electronic and steric substituents, as summarized in Scheme 2. Under the optimized conditions SGO (10 wt %, Table-1), ethanol medium, TBHP (1.2 equiv), and 80 °C. All evaluated substrates underwent seamless transformation into the respective benzimidazole derivatives (3a–j, Table-2) with good to exceptional isolated yields. From an electronic perspective, electron donating substituents on the aromatic ring (e.g., alkyl and alkoxy groups) generally facilitated the cyclization, affording products in slightly higher yields and shorter reaction times. This behaviour can be contributed to increased nucleophilicity of the amino functional group, which promotes the initial condensation with the *in situ* generated methine intermediate derived from glucose. In contrast, electron-withdrawing substituents (such as halogens or nitro groups) were also well tolerated, albeit requiring marginally longer reaction times, likely due to reduced electron density on the diamine nitrogen atoms. Importantly, no competitive over-oxidation or ring degradation was observed even in strongly electron-deficient systems, highlighting the mild yet effective oxidative environment provided by the SGO/TBHP combination. Steric effects were found to have a limited impact on the reaction outcome. Substrates containing substituents proximal to the amino functionalities still underwent efficient cyclization, indicating that the heterogeneous Brønsted-acidic surface of SGO effectively orients and activates the reacting partners at the solid–liquid interface. The reaction also demonstrated excellent functional group tolerance, accommodating halides, alkyl, and aryl substituents without interference, which is particularly advantageous for downstream derivatization.

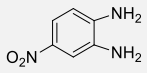
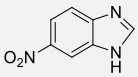
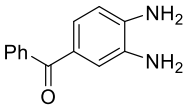
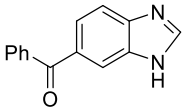
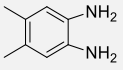
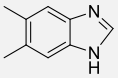
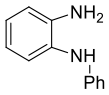
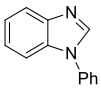
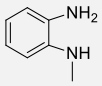
Mechanistically, the reaction is proposed to proceed *via* the SGO-assisted generation of an electrophilic methine (–CH–) species from glucose under oxidative conditions, followed by sequential C–N bond formation and intramolecular cyclization of the *o*-phenylenediamine substrate. The presence of sulfonic acid groups on SGO plays a dual role: (i) activating glucose toward controlled oxidative fragmentation and (ii) promoting dehydration and aromatization steps leading to the benzimidazole core. Ethanol serves not only as a green solvent but also facilitates proton transfer steps, while TBHP acts as a benign terminal oxidant.

Notably, the heterogeneous catalyst could be readily recovered by simple filtration and reused in multiple cycles with minimal loss of activity, confirming the operational stability of the sulfonated graphene oxide under aqueous oxidative conditions. The exclusive formation of benzimidazole products, without detectable side products, underscores the high chemo-selectivity of the protocol.

Overall, the reaction scope study establishes this methodology as a general, sustainable, and scalable approach for the synthesis of structurally diverse benzimidazoles. The combination of renewable glucose as a C_1 source, ethanol as solvent, metal-free conditions, and a recyclable nanocatalyst makes this transformation particularly attractive from both green chemistry and synthetic utility perspectives.

Table 2. SGO catalysed cyclization of *o*-phenylenediamine with D-glucose for Benzimidazoles Derivatives

S. No.	Substrate	Final Product	% Yield
1a	 **1a**	 **3a**	91
2	 **1b**	 **3b**	93
3	 **1c**	 **3c**	87
4	 **1d**	 **3d**	88
5	 **1e**	 **3e**	90

6	 1f	 3f	88
7	 1g	 3g	91
8	 1h	 3h	87
9	 1i	 3i	92
10	 1j	 3j	88

4.2 Recycling of SGO nanocatalyst

Under the best reaction conditions, the SGO reusage was severely examined (Table 1, Entry 17). After the targeted reaction was completed, the catalyst was recovered by filtration, washed with fresh DI water and MeOH, and dried for 1.5 hours at 120°C in a hot air oven. Fig. 9 shows a graphic representation of the conversion for each of the four cycles (Brahmayya *et al.* 2018).

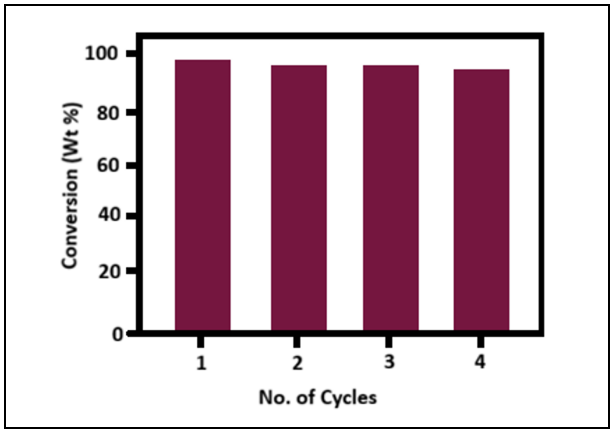


Fig. 9: Recycle of the nano catalyst SGO

4.3 Antimicrobial Activity

The newly synthesized organic molecules were screened for their antibacterial activity (Table 3) against gram positive bacteria *Staphylococcus aureus* and Streptococcus pyogenes and gram-negative bacteria *Escherichia coli* and *Pseudomonas aeruginosa*. Antibacterial activity was carried out by serial broth dilution method. The standard strains used for the antimicrobial activity were procured from the IMT, Chandigarh, India. Compounds (3a–j) were screened for their antibacterial activity (Rehman *et al.* 2025; Ibrahim *et al.* 2025 and Alagoz, 2016) in triplicate *against E. coli, S. aureus, P. aeruginosa,* and *S. pyogenes*. The drugs which were found to be active in primary screening were diluted to obtain required concentrations to get more close result. The growths of bacterial cultures were monitored after 24 and 48 hours. The lowest concentration, which showed no growth after spot sub culture was considered as MIC for each drug. Also, the highest dilution showing at least 99.99-100 % inhibition is taken as MIC. The test mixture selected for this assay contained 10^8 cells/mL. The standard drug used for this study was Chloramphenicol against *E. coli, P. aeruginosa, S. aureus,* and *S. pyogenes,* respectively. Further, synthesized compounds 3b, 3d, 3e, 3f exhibited exceptional high biological activity (Table 3) due to the presence of active functional groups such as fluorine (Table 3, compound 3b, inhibition rate 99.88-100%), bromine (Table 3, compound 3d, inhibition rate 99.70-99.99%), chlorine (Table 3, compound 3e, inhibition rate 98.90-99.88%), nitro group (Table 3, compound 3f, inhibition rate (100%). In addition, active functional groups with electron withdrawing nature increases the reactivity of molecules and binding capability towards bacteria. The remaining compounds could not show much better antimicrobial activity due to presence of inactive functional groups in organic molecules (Fig. 10).

Table 3. Antibacterial activity of compounds (3a–j)

Prepared Compound	R/R1	Bacterial strains			
		E. coli	*P. aeruginosa*	*S. aureus*	*S. pyogenes*
		Rate of inhibition (%)			
3a	H	87.00	88.00	90.00	88.00
3b	6–F	99.99	99.98	100	99.88
3c	6–CH_3	96.90	97.30	95.90	96.30
3d	6–Br	99.99	99.70	99.78	99.70
3e	6–Cl	99.00	99.60	99.88	98.90
3f	6-NO_2	100	100	100	100
3g	6-COC_6H_5	94.00	96.00	96.99	98.00
3h	5,6-CH_3	88.01	91.00	87.23	91.08
3i	1-C_6H_5	91.60	92.30	96.89	94.31
3j	1-CH_3	87.00	86.00	86.88	87.00
Standard Drug	Chloramphenicol (Antibiotic)	100	100	100	100

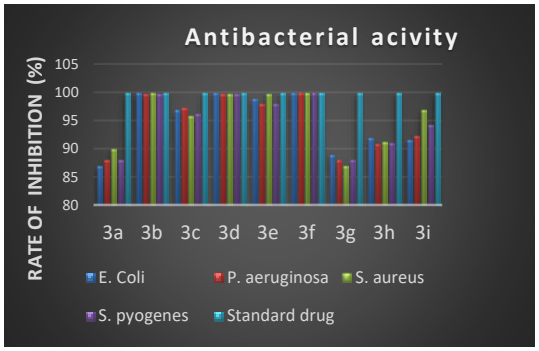


Fig. 10: Graphical representation of antibacterial activity of synthesised compounds

5. CONCLUSIONS

Sulfonated graphene oxide possesses notable properties, including a large surface area, a high density of acidic sites, and excellent dispersibility, making it a promising material for applications in nanocatalysis. In this study, SGO was synthesized and characterized for use in organic transformations. Graphene oxide was first prepared by oxidizing graphite powder, followed by sulfonation using *p*-diazobenzenesulfonic acid under ultrasonic treatment to obtain SGO. The synthesized nanocatalyst was then applied to the preparation of benzimidazole derivatives. Initially, o-phenylenediamine and D-glucose were used as starting substrates to synthesize the target compounds. The antibacterial activity of the resulting benzimidazole derivatives was evaluated against bacterial strains, including *P. aeruginosa*, *E. coli*, *S. aureus*, and *S. pyogenes*. The compounds exhibited excellent antibacterial activity, with inhibition rates ranging from 99.99% to 100%.

ACKNOWLEDGEMENTS

All authors have equally contributed to this research work and the manuscript. Author M.V.M is grateful to Dr. MB for his supervision and assisting in the characterization of the catalysts. Manuscript was drafted by M.V.M and reviewed and revised by Dr. MB, Dr. MP.

FUNDING

This research received no specific grant from any funding agency in the public, commercial, or not-for-profit sectors.

CONFLICTS OF INTEREST

The authors declare that there is no conflict of interest.

COPYRIGHT

This article is an open-access article distributed under the terms and conditions of the Creative Commons Attribution (CC BY) license (http://creativecommons.org/licenses/by/4.0/).

REFERENCES

Alagoz, A. Z., Antimicrobial activities of 1-H-benzimidazole-based molecules, *Curr. Topics Med. Chem.,* 16(26), 2953-2962 (2016). https://doi.org/10.2174/1568026616666160506130226

Alminderej, F. M. and Lotfi, A., Design, synthesis, characterization and anticancer evaluation of novel mixed complexes derived from 2-(1H-Benzimizadol-2-yl) aniline Schiff base and 2-mercaptobenzimidazole or 2-aminobenzothiazole, *Egypt. J. Chem.,* 64(7), 3351-3364 (2021). https://doi.org/10.21608/ejchem.2021.60640.3305

Azmiyawati, C., Ridha, J. S. and Bima, D. N., Synthesis of sulfonated graphene oxide (SGO) using reflux method for adsorption of Cr (VI) metal ions, *AIP Conf. Proc.,* 3166(1), 020037 (2025). https://doi.org/10.1063/5.0236990

Baars, H., Beyer, A., Kohlhepp, S. V. and Bolm, C., Transition-metal-free synthesis of benzimidazoles mediated by KOH/DMSO, *Org. lett.,* 16(2), 536-539 (2014). https://doi.org/10.1021/ol403414v

Bansal, Y. and Silakari, O., The therapeutic journey of benzimidazoles: A review, *Bioorg. Med. chem.,* 20(21), 6208-6236 (2012). https://doi.org/10.1016/j.bmc.2012.09.013

Barker, H. A., Smyth, R. D., Weissbach, H., Toohey, J. I., Ladd, J. N. and Volcani, B. E., Isolation and properties of crystalline cobamide coenzymes containing benzimidazole or 5, 6-dimethylbenzimidazole, *J. Biol. Chem*., 235(2), 480-8 (1960). https://doi.org/10.1016/S0021-9258(18)69550-X

Basak, P., Dey, S. and Ghosh, P., Sulfonated Graphene-Oxide as Metal-Free Efficient Carbocatalyst for the Synthesis of 3-Methyl-4-(hetero) arylmethylene isoxazole-5 (4H)-ones and Substituted Pyrazole, *Chem. Select,* 5(2), 626-636 (2020). https://doi.org/10.1002/slct.201904164

Bastug, G., Eviolitte, C. and Marko, I. E., Functionalized orthoesters as powerful building blocks for the efficient preparation of heteroaromatic bicycles, *Org. Lett.,* 14(13), 3502-3505 (2012). https://doi.org/10.1021/ol301472a

Brahmayya, M., Dai, S. A. and Suen, S. -Y., Facile synthesis of 2-benzimidazolones via carbonylation of o-phenylenediamines with CO2, *J. CO2 Util.,* 22, 135-142 (2017). https://doi.org/10.1016/j.jcou.2017.09.006

Brahmayya, M., Dai, S. A. and Suen, S. Y., Synthesis of 5-substituted-3 H-[1, 3, 4]-oxadiazol-2-one derivatives: a carbon dioxide route (CDR), *RSC adv.,* 5(80), 65351-65357 (2015). https://doi.org/10.1039/C5RA08910G

Brahmayya, M., Suen, S. Y. and Dai, S. A., Sulfonated graphene oxide-catalyzed N-acetylation of amines with acetonitrile under sonication, *J. Taiwan Inst. Chem. Eng.,* 83, 174-183 (2018). https://doi.org/10.1016/j.jtice.2017.12.003

Brahmayya, M., Suen, S. Y. and Dai, S. H. A., Sulfonated reduced graphene oxide catalyzed cyclization of hydrazides and carbon dioxide to 1,3,4-oxadiazoles under sonication, *Sci. Rep.,* 7, 4675 (2017). https://doi.org/10.1038/s41598-017-04143-4

Cao, N., Zhou, C., Wang, Y., Ju, H., Tan, D., Li, J., Synthesis and characterization of sulfonated graphene oxide reinforced sulfonated poly (ether ether ketone)(SPEEK) composites for proton exchange membrane materials, *Mater.,* 11(4), 516 (2018). https://doi.org/10.3390/ma11040516

Chen, H. Y., Kulkarni, M. V., Chen, C. H. and Sun, C. M., Synthesis of structurally diverse benzimidazolyl benzimidazolones by application of soluble polymer support, *Tetrahedron,* 64(27), 6387-6394 (2008). https://doi.org/10.1016/j.tet.2008.04.081

Daripa, S., Singh, V. K., Prakash, O., Maiti, P., Kuila, B. K. and Das, S., Sulfonated graphene-modified electrodes for enhanced capacitive performance and improved electro-oxidation of hydrogen peroxide, *Nano-Struct. Nano-Obj.,* 24,100531 (2020). https://doi.org/10.1016/j.nanoso.2020.100531

Desai, N. C., Pandya, D. D., Joshi, V. V., Rajpara, K. M., Vaghani, H. V. and Satodiya, H. M., Synthesis, characterization and antimicrobial screening of hybrid molecules containing benzimidazole-pyrazole and pyridine nucleus, *Med. Chem. Res.,* 21(12), 4463-4472 (2012). https://doi.org/10.1007/s00044-012-9990-4

Desai, N. C., Pandya, D. D., Kotadiya, G. M. and Desai, P., Synthesis and characterization of novel benzimidazole bearing pyrazoline derivatives as potential antimicrobial agent, *Med. Chem. Res.,* 23(3), 1474-1487 (2014). https://doi.org/10.1007/s00044-013-0756-4

Ding, S. and Jiao, N. N., N-dimethylformamide: A multipurpose building block, *Angewandte Chem. Int. Ed.,* 51(37), 9226-9237 (2012). https://doi.org/10.1002/anie.201200859

Dudd, L. M., Venardou, E., Garcia-Verdugo, E., Licence, P., Blake, A. J., Wilson, C. and Poliakoff, M., Synthesis of benzimidazoles in high-temperature water, *Green Chem.,* 5(2), 187-192 (2003). https://doi.org/10.1039/B212394K

Farid, M. A., Lease, J. and Andou, Y., Temperature-dependent deoxygenation during sulfonation for graphene oxide reduction, *Appl. Surf. Sci.,* 691, 162678 (2025). https://doi.org/10.1016/j.apsusc.2025.162678

Francesconi, V., Cichero, E., Schenone, S., Naesens, L. and Tonelli, M., Synthesis and biological evaluation of novel (thio) semicarbazone-based benzimidazoles as antiviral agents against human respiratory viruses, *Mol.,* 25(7), 1487 (2020). https://doi.org/10.3390/molecules25071487

Garfunkle, J., Ezzili, C., Rayl, T. J., Hochstatter, D. G., Hwang, I., Boger, D. L., Optimization of the central heterocycle of α-ketoheterocycle inhibitors of fatty acid amide hydrolase, *J. med. chem.,* 51(15), 4392-4403 (2008). https://doi.org/10.1021/jm800136b

Gaudino, E. C., Tagliapietra, S., Palmisano, G., Martina, K., Carnaroglio, D. and Cravotto, G., Microwave-Assisted, Green Synthesis of 4 (3 H)-Quinazolinones under CO Pressure in γ-Valerolactone and Reusable Pd/β-Cyclodextrin Cross-Linked Catalyst, *ACS Sustainable Chem. Eng.,* 5(10), 9233-9243 (2017). https://doi.org/10.1021/acssuschemeng.7b02193

Hao, L., Zhao, Y., Yu, B., Zhang, H., Xu, H. and Liu, Z., Au catalyzed synthesis of benzimidazoles from 2-nitroanilines and CO 2/H 2, *Green Chem*., 16(6), 3039-3044 (2014). https://doi.org/10.1039/C4GC00153B

Hati, S., Dutta, P. K., Dutta, S., Munshi, P. and Sen, S., Accessing benzimidazoles via a ring distortion strategy: an oxone mediated tandem reaction of 2-Aminobenzylamines, *Org. lett.,* 18(13), 3090-3093 (2016). https://doi.org/10.1021/acs.orglett.6b01217

Huang, J., Chen, Z. and Wu, J., Recent Progress in Methyl-Radical-Mediated Methylation or Demethylation Reactions, *ACS Catal.,* 11(17), 10713-10732 (2021). https://doi.org/10.1021/acscatal.1c02010

Ibrahim, A. A., Said, E. G., AboulMagd, A. M., Amin, N. H. and Abdel-Rahman, H. M., Synthesis and SARs of benzimidazoles: insights into antimicrobial innovation (2018–2024), *RSC adv.,* 15(27), 22097-22127 (2025). https://doi.org/10.1039/D5RA00819K

Kang, S., Moon, H. K., Yoon, Y. -J. and Yoon, H. J., Recent Progress in the Chemistry of Pyridazinones for Functional Group Transformations, *J. Org. Chem.,* 83 (1), 1-11 (2018). https://doi.org/10.1021/acs.joc.7b02481

Kattimani, P. P., Kamble, R. R. and Meti, G. Y., Expedient synthesis of benzimidazoles using amides, *RSC Adv.,* 5(37), 29447-29455 (2015). https://doi.org/10.1039/C5RA00021A

Khan, M. T., Choudhary, M. I., Khan, K. M. and Rani, M., Structure–activity relationships of tyrosinase inhibitory combinatorial library of 2, 5-disubstituted-1, 3, 4-oxadiazole analogues, *Bioorg. Med. Chem.,* 13(10), 3385-3395 (2005). https://doi.org/10.1016/j.bmc.2005.03.012

Kovvuri, J., Nagaraju, B., Kamal, A. and Srivastava, A. K., An Efficient Synthesis of 2-Substituted Benzimidazoles via Photocatalytic Condensation of o-Phenylenediamines and Aldehydes, *ACS Comb. Sci.,* 18(10), 644-650 (2016). https://doi.org/10.1021/acscombsci.6b00107

Krishna, M. M. V., Brahmayya, M., Deepthi, S., Harinath, A., Buddiga, L. R., Rao, J. C. S., Padma, M., Choppara, P., Samsonu, D. and Rao, A. V., Sulfonated Graphene Oxide Catalyzed Transformation of Pyrazole-Oxazolidine Derivatives and Their Antimicrobial Activities, *Asian J. Chem.,* 38, 180-186 (2025). https://doi.org/10.14233/ajchem.2026.34993

Krishna, M. V. M., Rao, J. C., Kothapalli, S. S., Brahmayya, M., Vineela, K. C., Rao, K. T., Marupati, S., Padma, M. and Indla, S., Sulfonated grapheneoxide as a sustainable metal free acid catalyst: a smart approach for synthesizing 1, 3, 4-oxadiazole derivatives from carboxylic acids: antimicrobial activities, *Disc. Catal.,* 2(1), 14 (2025). https://doi.org/10.1007/s44344-025-00018-3

Kudale, V. S. and Wang, J. J., Metal-free C–H methylation and acetylation of heteroarenes with PEG-400, *Green Chem.,* 22(11), 3506-3511 (2020). https://doi.org/10.1039/D0GC01183E

Li, C. J. and Chen, L., Organic chemistry in water, *Chem. Soc. Rev.,* 35(1), 68-82 (2006). https://doi.org/10.1039/B507207G

Li, H., Guo, H., Fang, Z., Aida, T. M., Smith and R. L., Cycloamination strategies for renewable N-heterocycles, *Green Chem*., 22(3), 582-611 (2020). https://doi.org/10.1039/C9GC03655E

Li, Z., Song, H., Guo, R., Zuo, M., Hou, C., Sun, S., He, X., Sun, Z. and Chu, W., Visible-light-induced condensation cyclization to synthesize benzimidazoles using fluorescein as a photocatalyst, *Green Chem.,* 21(13), 3602-3605 (2019). https://doi.org/10.1039/C9GC01359H

Lin, J. P., Zhang, F. H. and Long, Y. Q., Solvent/oxidant-switchable synthesis of multisubstituted quinazolines and benzimidazoles via metal-free selective oxidative annulation of arylamidines, *Org. lett.,* 16(11), 2822-2825 (2014). https://doi.org/10.1021/ol500864r

Liu, W., Yang, X., Zhou, Z. Z. and Li, C. J., Simple and clean photo-induced methylation of heteroarenes with MeOH, *Chem.,* 2(5), 688-702 (2017). http://doi.org/10.1016/j.chempr.2017.03.009

Ma, X., Su, J., Zhang, X. and Song, Q., Chlorodifluoromethane as a C1 Synthon in the Assembly of N-Containing Compounds, *Isci*., 27, 19:1-13 (2019). http://doi.org/10.1016/j.isci.2019.07.005

Mahesh, D., Sadhu, P. and Punniyamurthy, T., Copper (II)-catalyzed oxidative cross-coupling of anilines, primary alkyl amines, and sodium azide using TBHP: A route to 2-substituted benzimidazoles, *J. Org. Chem.,* 81(8), 3227-3234 (2016). https://doi.org/10.1021/acs.joc.6b00186

Marinescu, M., Synthesis of antimicrobial benzimidazole–pyrazole compounds and their biological activities, *Antibiot.,* 10(8), 1002 (2021). https://doi.org/10.3390/antibiotics10081002

Mayo, M. S., Yu, X., Zhou, X., Feng, X., Yamamoto, Y. and Bao, M., Convenient synthesis of benzothiazoles and benzimidazoles through Brønsted acid catalyzed cyclization of 2-amino thiophenols/anilines with β-diketones, *Org. lett.,* 16(3), 764-767 (2014). https://doi.org/10.1021/ol403475v

Mohammadi, O., Golestanzadeh, M. and Abdouss, M., Recent advances in organic reactions catalyzed by graphene oxide and sulfonated graphene as heterogeneous nanocatalysts: a review, *New J. Chem.,* 41(20), 11471-11497 (2017). https://doi.org/10.1039/C7NJ02515G

Mutra, M. R., Dhandabani, G. K. and Wang, J. -J., Mild Access to N-Formylation of Primary Amines using Ethers as C1 Synthons under Metal-Free Conditions, *Adv. Synth. Catal.,* 360(20), 3960-3968 (2018). https://doi.org/10.1002/adsc.201800783

Natte, K., Neumann, H., Jagadeesh, R. V. and Beller, M., Convenient iron-catalyzed reductive aminations without hydrogen for selective synthesis of N-methylamines, *Nat. Commun*., 8(1), 1344 (2017). https://doi.org/10.1038/s41467-017-01428-0

Nguyen, T. B., Ermolenko, L., Dean, W. A. and Al-Mourabit, A., Benzazoles from aliphatic amines and o-amino/mercaptan/hydroxyanilines: elemental sulfur as a highly efficient and traceless oxidizing agent, *Org. lett.,* 14(23), 5948-5951 (2012). https://doi.org/10.1021/ol302856w

Nguyen, T. B., Le Bescont, J., Ermolenko, L. and Al-Mourabit, A., Cobalt-and iron-catalyzed redox condensation of o-substituted nitrobenzenes with alkylamines: a step-and redox-economical synthesis of diazaheterocycles, *Org. lett.,* 15(24), 6218-6221 (2013). https://doi.org/10.1021/ol403064z

Peng, J. -B., Wu, Fu. -P. and Wu, X. F., First-Row, Transition-Metal-Catalyzed Carbonylative Transformations of Carbon Electrophiles, *Chem. Rev.,* 119 (4), 2090–2127 (2019). https://doi.org/10.1021/acs.chemrev.8b00068

Rajora, J. and Srivastava, Y. K., Synthesis and antimicrobial activities of some benzimidazolyl pyrazoles, *Rasayan J. Chem.,* 2(3), 655-658 (2009). https://www.rasayanjournal.co.in/vol-2/issue-3/20.pdf

Refat, M. S., Hamza, R. Z., Adam, A. M. A., Saad, H. A., Gobouri, A. A., Al-Salmi, F. A., Altalhi, T. and El-Megharbel, S. M., Synthesis of N, N′-bis (1, 5-dimethyl-2-phenyl-1, 2-dihydro-3-oxopyrazol-4-yl) sebacamide that ameliorate osteoarthritis symptoms and improve bone marrow matrix structure and cartilage alterations induced by monoiodoacetate in the rat model:"Suggested potent anti-inflammatory agent against COVID-19, *Human Exp. Toxicol.,* 40(2), 325-341 (2021). https://doi.org/10.1177/0960327120945779

Rehman, M. U., He, F., Shu, X., Guo, J., Liu, Z., Cao, S. and Long, S., Antibacterial and antifungal pyrazoles based on different construction strategies, *Europ. J. Med. Chem.,* 282, 117081 (2025). https://doi.org/10.1016/j.ejmech.2024.117081

Ryu, K. E., Kim, B. R., Sung, G. H., Yoon, H. J. and Yoon, Y. -J., Facile Synthesis of Benzo[d]azol-2(3H)-ones Using 2-Phenoxycarbonyl-4,5-dichloropyridazin-3(2H)-one as Green CO Source, *Synlett,* 26 (14), 1985–1990 (2015). https://doi.org/10.1055/s-0034-1378783

Senadi, G. C., Mutra, M. R., Lu, T. Y. and Wang, J. J., Oximes as reusable templates for the synthesis of ureas and carbamates by an in situ generation of carbamoyl oximes, *Green Chem.,* 19(18), 4272-4277 (2017). https://doi.org/10.1039/C7GC01449J

Sun, Z., Bottari, G. and Barta, K., Supercritical methanol as solvent and carbon source in the catalytic conversion of 1, 2-diaminobenzenes and 2-nitroanilines to benzimidazoles, *Green Chem.,* 17(12), 5172-5181 (2015). https://doi.org/10.1039/C5GC01040C

Tchekep, A. K., Suryanarayanan, V. and Pattanayak, D. K., Simultaneous synthesis of sulfonated reduced graphene oxide@ graphene oxide hybrid material for efficient electrochemical sensing of silver ions in drinking water, *Carbon Trends.,* 16, 100393 (2024). https://doi.org/10.1016/j.cartre.2024.100393

Wang, S. and Xi, C., Recent advances in nucleophile-triggered CO2-incorporated cyclization leading to heterocycles, *Chem. Soc. Rev.,* 48 (1), 382–404 (2019). https://doi.org/10.1039/C8CS00281A

Wei, Y., Wu, J., Xue, D., Wang, C., Liu, Z., Zhang, Z., Chen, G. and Xiao, J., Highly efficient rhodium-catalyzed transfer hydrogenation of nitroarenes into amines and formanilides, *Synlett.,* 25(09), 1295-1298 (2014). https://doi.org/10.1055/s-0033-1341250

Xu, X., Huang, L., Yin, X., Eycken, E. V. V. d. and Feng, H., Dual roles of ynoates: desymmetrization of dicarboxylic acids using trialkylamines as alkyl equivalents, *Org. Chem. Front.,* 5(20), 2955-2959 (2018). https://doi.org/10.1039/C8QO00919H

Yu, B., Zhang, H., Zhao, Y., Chen, S., Xu, J., Hao, L. and Liu, Z., DBU-based ionic-liquid-catalyzed carbonylation of o-phenylenediamines with CO2 to 2-benzimidazolones under solvent-free conditions, *ACS Catal.,* 3(9), 2076-2082 (2013). https://doi.org/10.1021/cs400256j

Yu, H., Jin, Y., Li, Z., Peng, F. and Wang, H., Synthesis and characterization of sulfonated single-walled carbon nanotubes and their performance as solid acid catalyst, *J. Solid State Chem*., 181(3), 432-438 (2008). https://doi.org/10.1016/j.jssc.2007.12.017

Zahid, M., Rashid, A., Akram, S., Shakir, H. F., Rehan, Z. A., Javed, T., Shabbir, R. and Hessien, M. M., Fabrication and characterization of sulfonated graphene oxide-doped polymeric membranes with improved anti-biofouling behavior, *Memb.,* 11(8), 563 (2021). https://doi.org/10.3390/membranes11080563

Zhang, Y., Feng, J., Li and C. J., Palladium-catalyzed methylation of aryl C− H bond by using peroxides, *J. Am. Chem. Soc.,* 130(10), 2900-29001 (2008). https://doi.org/10.1021/ja0775063

Zhang, Z., Sun, Q., Xia, C. and Sun, W., CO2 as a C1 source: B (C6F5) 3-catalyzed cyclization of o-phenylene-diamines to construct benzimidazoles in the presence of hydrosilane, *Org. lett.,* 18(24), 6316-6319 (2016). https://doi.org/10.1021/acs.orglett.6b03030